Intracellular routing of β-catenin
Hendriksen, J.V.R.B.

Citation
Hendriksen, J. V. R. B. (2008, June 19). *Intracellular routing of β-catenin*.
Retrieved from https://hdl.handle.net/1887/12965

Chapter 4

Plasma membrane recruitment of signaling-competent ß-catenin upon activation of the Wnt pathway

4

Plasma membrane recruitment of signaling competent ß-catenin upon activation of the Wnt pathway

Jolita Hendriksen[1,5], Marnix Jansen[1,2,5], Carolyn M. Brown[4],
Hella van der Velde[1], Marco van Ham[3], Niels Galjart[3], G. Johan Offerhaus[2],
Francois Fagotto[4] and Maarten Fornerod[1]

1 Dept. of Tumor Biology, The Netherlands Cancer Institute, Plesmanlaan 121, 1066 CX Amsterdam, The Netherlands
2 Department of Pathology, University Medical Center Utrecht, 3584 ZX Utrecht, The Netherlands
3 Dept. of Cell Biology, Erasmus MC, Dr. Molewaterplein 50, 3015 GE Rotterdam, The Netherlands
4 Department of Biology, McGill University,1205 Dr. Penfield Ave., Montreal, QC H3A 1B1, Canada
5 These authors contributed equally to this work

The standard model of Wnt signaling specifies that after receipt of a Wnt ligand at the membrane-associated receptor complex, downstream mediators inhibit a cytoplasmic destruction complex, allowing ß-catenin to accumulate in the cytosol and nucleus and co-activate Wnt target genes. Unexpectedly, upon Wnt treatment, we detected the dephosphorylated form of ß-catenin at the plasma membrane, displaying a discontinuous punctate labeling. This pool of ß-catenin could only be detected in E-cadherin (-/-) cells, because in E-cadherin (+/+) cells Wnt-induced, membrane-associated ß-catenin was concealed by a constitutive junctional pool. Wnt signaling-dependent dephosphorylated ß-catenin co-localized at the plasma membrane with members of the destruction complex APC and Axin and the activated Wnt co-receptor LRP6. ß-Catenin induced through the Wnt receptor complex was transcriptionally significantly more competent than overexpressed ß-catenin, both in cultured cells and in early Xenopus embryos. Our data reveal an unappreciated step in processing of the Wnt signal and suggest multiple levels of regulation of signaling output beyond the level of protein accumulation.

The Wnt pathway is a critical determinant of cell proliferation during development and regenerative processes such as stem cell proliferation in the adult (Clevers, 2006). Aberrant activation of the pathway has been linked to oncogenesis in multiple systems. A central player in the Wnt pathway is ß-catenin. Most of the cellular pool of ß-catenin is tethered to E-cadherin (encoded by the Cdh1 gene) as an adherens junction component mediating cell-cell adhesion (McCrea et al., 1991; Peifer et al., 1994a). A less abundant pool of ß-catenin, often referred to as the 'free' pool of ß-catenin, functions in complex with TCF/Lef transcription factors as a transcriptional co-activator of Wnt signaling in the nucleus (Cadigan and Nusse, 1997). In the absence of a Wnt signal, the free pool of ß-catenin is tightly regulated through phosphorylation at specific N-terminal residues by a so-called 'destruction complex' consisting of the serine kinases CK1α and GSK3 and the tumor suppressors Adenomatous Polyposis Coli (APC) and Axin (Logan and Nusse, 2004). Phosphorylated ß-catenin is marked for rapid ubiquitinization and degradation by the proteasome. Receipt of a Wnt ligand at the membrane-associated receptor complex results in inhibition of ß-catenin breakdown, allowing ß-catenin to accumulate, enter the nucleus and activate a Wnt target gene program (Logan and Nusse, 2004).

However, our current understanding of Wnt signal transduction and ß-catenin processing suffers from significant gaps. In particular, the make-up and subcellular localization of the mature destruction complex is unclear at present. For this reason, the mechanism through which the destruction complex senses ligand engagement at the Frizzled/LRP receptor complex remains unidentified. Recently, increasing evidence suggests important regulatory steps in the turnover of the destruction complex may take place at the plasma membrane (for a review see Cadigan and Liu, 2006). Engagement of the Frizzled and LRP5/6 co-receptors on the cell surface by Wnt ligands, results in the phosphorylation of the intracellular domain of LRP5/6 by CK1γ and/or GSK3ß. Phosphorylated LRP5/6 presents a docking site for Axin that is recruited to the plasma membrane in response to Wnt stimulation (Cliffe et al., 2003; Davidson et al., 2005; Zeng et al., 2005) along with other canonical Wnt pathway components including Axin, GSK3ß and Fz8 (Bilic et al., 2007). The scaffold protein dishevelled (Dvl) appears to be required for this trans-

4

location (Schwarz-Romond et al., 2007). Although it remains unproven, it has been hypothesized that cytoplasmic destruction of ß-catenin is halted as a result of Axin relocation, allowing ß-catenin to redistribute to the nucleus.

Nuclear localization of ß-catenin is considered a hallmark of Wnt activation, yet in many systems it is only incidentally detected in the nucleus (Anderson et al., 2002; Kobayashi et al., 2000). The nuclear level of the N-terminally dephosphorylated (or 'dephospho') form of ß-catenin has been shown to correlate much better with Wnt activity (Staal et al., 2002). Dephospho-ß-catenin has been suggested to reflect the *de novo* translated form of ß-catenin, which is involved in signal transduction (Willert et al., 2002). We set out to optimize experimental conditions for the detection of dephospho-ß-catenin in cultured mammalian cell lines. In a series of colon carcinoma cell lines, dephospho-ß-catenin often localizes to the plasma membrane. Although we find no correlation with either APC or ß-catenin mutation status, the plasma membrane localization of dephospho-ß-catenin does correlate with E-cadherin expression. Surprisingly, stimulation of E-cadherin -/- cells with Wnt3A resulted in the appearance of dephospho-ß-catenin at the plasma membrane, where it co-localizes with the activated form of LRP6, APC and Axin. By unmasking the transcriptionally competent pool of ß-catenin, we provide evidence for a key step in ß-catenin processing and Wnt signal transduction at the plasma membrane.

Results

Dephospho-ß-catenin is present in cadherin complexes

Because N-terminally dephosphorylated ß-catenin represents a better marker for Wnt signaling activity than total ß-catenin, we optimized experimental conditions allowing detection of dephospho-ß-catenin by the α-ABC (8E7) antibody (van Noort et al., 2002) in cultured mammalian cell lines. This antibody specifically reacts with an N-terminally unphosphorylated peptide (amino acids 36-44) that contains the GSK3ß target residues S37 and T41 (van Noort et al., 2007). Reproducible detection of dephospho-ß-catenin with the α-ABC antibody was highly dependent on fixation and blocking conditions, and further improved after antigen retrieval (see Materials and Methods). Screening of a set of colon carcinoma cell lines using these conditions showed both nuclear and plasma membrane localization of dephospho-ß-catenin, depending on the cell line (Fig 1A, Chapter 3, this thesis). Although we found no correlation with ei-

ther APC or ß-catenin mutation status, the plasma membrane localization of dephospho-ß-catenin does correlate positively with E-cadherin expression (Fig 1, Chapter 3, this thesis).

Cadherin-independent plasma membrane localization of dephospho-ß-catenin upon Wnt3A stimulation

In order to eliminate E-cadherin expression as a confounding factor in our interpretation of endogenous Wnt-induced dephospho-ß-catenin accumulation, we turned to the murine mammary epithelial cell line Kep1, which does not express E-cadherin due to Cre-mediated recombination of both E-cadherin alleles, and compared it with its E-cadherin (+/+) isogenic control counterpart Kp6 (Derksen et al., 2006). In the absence of Wnt stimulation, these cell lines line do not activate a Wnt-responsive luciferase reportergene, indicating that these cell lines do not carry Wnt pathway activating mutations (Fig 1A). Earlier studies have demonstrated that in the presence of an intact destruction complex the loss of E-cadherin is neutral with respect to Wnt stimulation (van de Wetering et al., 2001). No or very little ß-catenin could be detected in unstimulated Kep1 cells. After 2.5 h stimulation with Wnt3A protein, however, a clear accumulation of the dephospho-ß-catenin form was seen (Fig 1B). In contrast, in the E-cadherin +/+ Kp6 cells dephospho-ß-catenin was clearly detected before Wnt stimulation (Fig1B).

In view of the transcriptional activation, we anticipated that in Wnt-stimulated Kep1 cells, dephospho-ß-catenin would be mainly nuclear. Surprisingly, stimulation of E-cadherin -/- Kep1 cells with Wnt3A resulted in the appearance of dephospho-ß-catenin at the plasma membrane (Fig. 1C). Nuclear staining of the ABC antibody is also observed. Note that this is partly aspecific, as some nuclear staining is also observed in unstimulated Kep1 cells and in NCI-H28 ß-catenin knock-out cells (data not shown), which is likely caused by a cross-reacting protein (in Fig. 1B marked by an asterisk). As expected, a similar plasma membrane accumulation in response to Wnt stimulation in E-cadherin -/- Kep1 cells is confirmed with antibodies to total ß-catenin (Fig. 2C). The discontinuous punctate plasma membrane labeling of dephospho-ß-catenin is strikingly similar to the plasma membrane-associated puncta described for LRP6-Axin (Bilic et al., 2007) and dishevelled (Dvl) (Schwarz-Romond et al., 2007) appearing upon Wnt treatment (see below). In unstimulated isogenic E-cadherin +/+ Kp6 cells dephospho-ß-catenin is prominent at the plasma membrane (Fig. 1C, right panel). This pool reflects transcriptionally
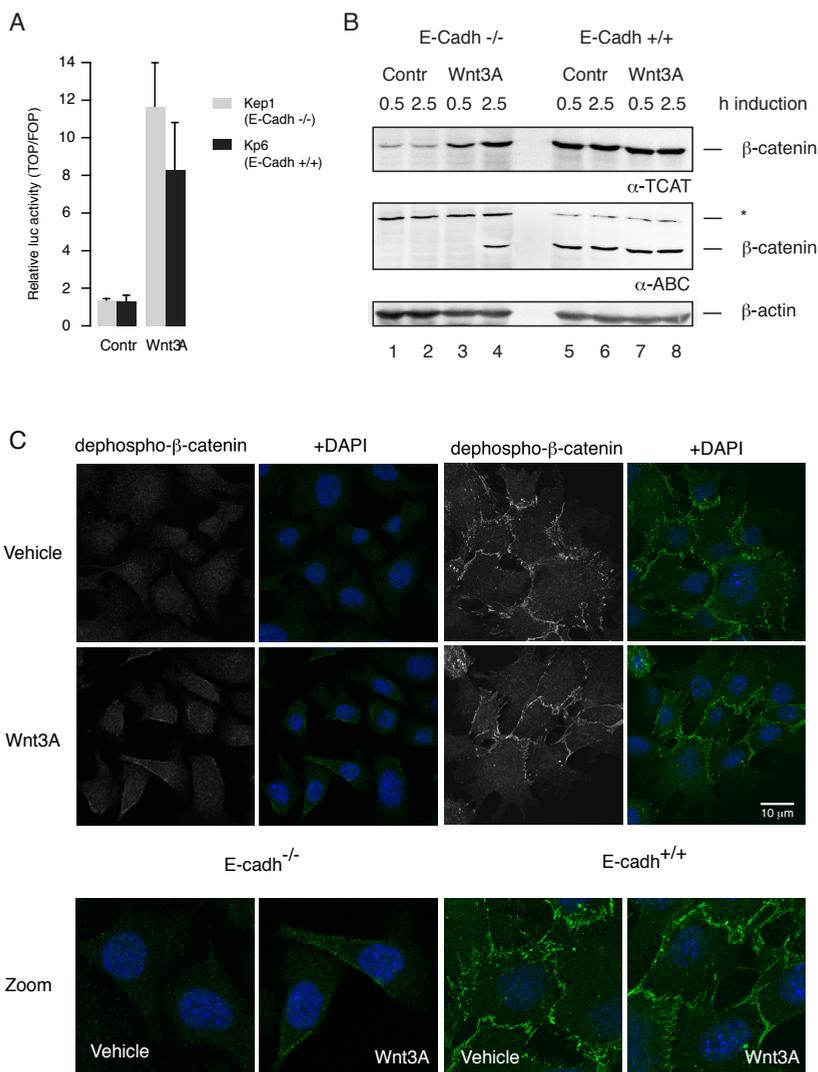
Figure 1. Cadherin-independent plasma membrane localization of dephospho-ß-catenin upon Wnt3A stimulation. A. E-cadherin negative cells respond normally to Wnt3a. Luciferase reporter assay in Kep1 (E-cadherin -/-) and Kp6 (E-cadherin +/+) cells using the TCF reporter TOP-TK and the control FOP-TK, normalized for transfection efficiency using pRL-CMV-Renilla. 24 Hours after transfection cells were stimulated overnight with Wnt3a conditioned or control medium and luciferase activity was measured. B. (Dephospho) ß-catenin levels in Kep1 or Kp6 cells. Cells were induced with Wnt3A protein or control and analyzed 0.5 or 2.5 h after induction by Western blotting using an antibody recognizing all forms of ß-catenin (α-TCAT) or an antibody specific for the N-terminal dephospho form (α-ABC). *, cross-reacting epitope. C. Subcellular localization of dephospho-ß-catenin in E-Cadherin positive or negative cells upon Wnt stimulation. Kep1 (E-cadherin -/-) or Kp6 (E-cadherin +/+) were induced with Wnt3A protein or control and analyzed 2.5 h after induction by immunolocalization with an antibody specific for the N-terminal dephospho form (α-ABC). DAPI was used as a nuclear marker. Note that dephospho-ß-catenin levels in E-cad -/- cells are much lower than in E-cad +/+ cells, requiring unequal confocal settings to be used.

inactive ß-catenin, as no reporter activity is detected (Fig. 1A). Wnt3A induces reporter activity in Kp6 (Fig. 1A), and a minor increase in signal is indeed detected on Western blot (Fig. 1B), but this increase does not translate in any noticeable increase in dephospho-ß-catenin staining in situ

(Figure 1C, right panel). This indicates that the signaling-competent dephospho-ß-catenin induced in response to Wnt stimulation is relatively minor in comparison to the steady-state junctional pool of dephospho-ß-catenin.

The absence of classical cadherins from Kep1 cells was confirmed using a 'pan-cadherin' antibody, which recognizes E, N and P cadherin. This antibody failed to show any membrane staining in Kep1 cells, neither before nor after Wnt3A stimulation (Supplementary Figure S1A). We wanted to further rule out the possibility that the recruitment of dephospho-ß-catenin to the plasma membrane could be the result of a Wnt-induced upregulation of a cadherin or another membrane protein acting as a cryptic docking site. Therefore, we studied the localization of dephospho-ß-catenin in Kep1 cells stimulated with Wnt3A protein, in the presence or absence of the transcription inhibitor actinomycin D. Under these conditions, ß-catenin was still stabilized and recruited to the plasma membrane (Supplementary Figure S1B), indicating that this process is independent of the induction of Wnt target genes.

Dephospho-ß-catenin colocalizes with APC, Axin and LRP6 at the plasma membrane after Wnt3A stimulation

Earlier studies have suggested translocation of members of the destruction complex to the LRP6 co-receptor upon Wnt signaling (Cliffe et al., 2003; Tolwinski et al., 2003). Phosphorylation on threonine 1479 of LRP6 is required for the recruitment of Axin and is carried out by CK1γ in response to Wnt signaling (Davidson et al., 2005). We therefore used a phospho-specific antibody recognizing this residue of LRP6 in immunofluorescence in Kep1 cells. We found that after stimulation with Wnt3A, phospho-LRP6 co-localized with dephospho-ß-catenin on the plasma membrane (Fig 2A). Likewise, we found that Axin colocalized with dephospho-ß-catenin (Fig 2B). These results suggest that the N-terminally dephosphorylated, or signaling-competent form, of ß-catenin is translocated to the receptor in a Wnt signaling-associated complex. Another component of the destruction complex, APC, has been reported to localize to the plasma membrane in different epithelial cell lines, including colon carcinoma cell lines (Miyashiro et al., 1995). As many available antibodies against APC are not reliable for immunofluorescence (Brocardo et al., 2005), we developed a monoclonal rat antibody, 3E7, that detects endogenous APC in immunofluorescence studies and on Western blot (Supplementary Figure S2). APC detected

with this antibody also clearly colocalized with ß-catenin on the membrane of Wnt3A stimulated Kep1 cells (Fig. 2C).

To further characterize the involvement of the Wnt receptor complex in recruitment of ß-catenin, we expressed ΔN-LRP6, a dominant active LRP6 receptor that mimics Wnt ligand engagement at the receptor complex. We could express this protein in SK-BR-3 cells, a breast cancer cell line with a homozygous deletion of E-cadherin (van de Wetering et al., 2001). Expression of this construct in Kep1 cells failed, since it was not properly presented at the plasma membrane in these cells (data not shown). As shown in Figure 2D, expression of ΔN-LRP6 resulted in a prominent plasma membrane localization of dephospho-ß-catenin, resembling the appearance of dephospho-ß-catenin in Kep1 cells at the plasma membrane after Wnt stimulation (Fig. 2A, B). This indicates that activation of LRP6 is involved in the E-cadherin-independent plasma membrane recruitment of dephospho-ß-catenin in response to Wnt signaling. Expression of ΔN-LRP6 in SK-BR-3 also resulted in colocalization of dephospho-ß-catenin with APC (Fig. 2E). We were unable to detect Axin in SK-BR-3 cells, possibly due to very low expression levels (data not shown). SK-BR-3 cells were found to be unresponsive to Wnt3A stimulation (data not shown) possibly due to the fact that these cells lack the appropriate Frizzled receptor for this ligand. We conclude that activation of the Wnt pathway by either Wnt3A or dominant active LRP6 leads to recruitment of Axin and/or APC and signaling competent ß-catenin to the plasma membrane.

LRP6-initiated dephospho-ß-catenin is transcriptionally significantly more competent than 'downstream-initiated' dephospho-ß-catenin

Our data so far are consistent with a model of Wnt signal transduction where, upon Wnt stimulation, *de novo* synthesized ß-catenin is attracted to the Wnt receptor complex together with members of the destruction complex. As Wnt activation results in co-activation of genes by ß-catenin in the nucleus, ß-catenin likely is released from the membrane complex and is routed to the nucleus. In order to test the relevance of membrane association of ß-catenin, we compared the activity of ß-catenin, either routed or not routed through the Wnt receptor complex. To mimic ß-catenin accumulation due to receptor activation we expressed ΔN-LRP6 in SK-BR-3 cells. To produce ß-catenin accumulation without receptor activation, we over-expressed wild-type ß-catenin. If the transactivating potential is similar regardless
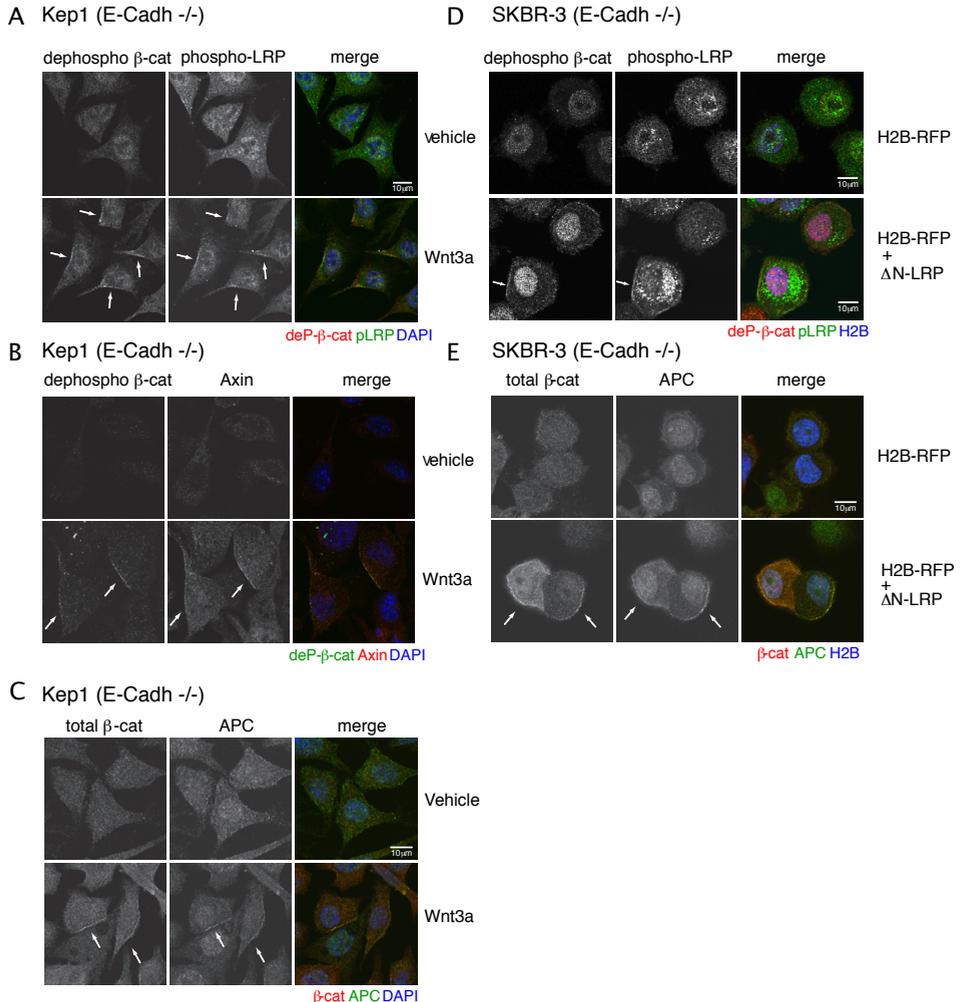
Figure 2. Dephospho-ß-catenin colocalizes with p-LRP6, Axin and APC at the plasma membrane in a Wnt-dependent (Kep1) or ∆N-LRP6 dependent (SK-BR-3) manner. Kep1 cells were induced with purified Wnt3A protein or vehicle for 2.5 h (Kep1), or transfected with ∆N-LRP6-encoding plasmid (SK-BR-3) and analyzed for subcellular localization of dephospho-ß-catenin and phospho-LRP6 (A and D), dephospho-ß-catenin and Axin (B), total ß-catenin and APC (C), and dephospho-ß-catenin and APC (E). Arrows denote plasma membrane localizations. Merged images are also shown that include DAPI as a nuclear marker (A-C) or H2B-mRFP as a transfection marker (D and E).

the source of dephospho-ß-catenin, the amount of luciferase output is expected to closely parallel the amount of dephospho-ß-catenin generated. As shown in Fig. 3, expression of ∆N-LRP6 resulted in significant upregulation of a lucifease reporter gene (Fig. 3C). A similar degree of TCF-reporter activation could be produced by transfection of wild-type ß-catenin, but this was accompanied by much higher cellular levels of dephospho-ß-catenin (Fig. 3D and E). Also, there was no enrichment of dephospho-ß-catenin on the plasma membrane under these conditions (Fig. 3B), while a prominent plasma membrane localization of the comparatively minor pool of dephospho-ß-catenin was induced by ∆N-LRP6 (Fig. 3A). Thus, in spite of significantly lower cellular levels of dephospho-ß-catenin, a similar degree of TCF reporter output can be achieved through LRP6 co-receptor activation.

Supraphysiological levels of exogenous ß-catenin are required to mimic Wnt activity in *Xenopus* embryos

We sought to support these observations in a second model. Wnt signaling activity in the early *X. laevis* embryo can be readily monitored by the formation of an ectopic body axis. We thus compared the levels of exogenously expressed ß-catenin required to induce secondary axes, to the levels produced by the endogenous dorsalizing center, or by a much stronger activation of the pathway by ectopic Wnt expression (Fig. 4G).

The endogenous Wnt pathway is active in the blastula (stage 8.5-9.5) and can be detected as

dephospho-β-catenin   H2B-mRFP

A

ΔN-LRP

dephospho-β-catenin   H2B-mRFP

B

β-cat (50 ng)

C

D

E

Figure 3. LRP6-initiated dephospho-ß-catenin is transcriptionally more active than downstream-initiated dephospho-ß-catenin. Cadherin-deficient SK-BR-3 breast carcinoma cells were transiently transfected with 25 or 50 ng plasmid encoding wild-type ß-catenin or 160 ng of a plasmid encoding ΔN-LRP6 and in parallel analyzed by immunolocalization (A and B), TCF transcriptional activity (C) and Western blotting (D and E). A-B. Immunolocalization of dephospho-ß-catenin in cells exogenously expressing ß-catenin or ΔN-LRP6, identified by co-expression of mRFP-tagged histone H2B. C. TCF-dependent transcriptional activity in SK-BR3 cells transfected with indicated plasmids 24 hours after transfection. TOP, TCF-reporter luciferase activity; FOP, mutated TCF-reporter activity. Values were normalized to a transfection control (constitutive Renilla luciferase reporter). D-E, Western blot analysis of cells shown in A-C, detecting total (D) or dephospho-ß-catenin (E) levels. 4x, four fold loaded; 0.5x, one half loaded.

Figure 4. Supraphysiological levels of exogenous ß-catenin are required to mimic Wnt activity in *Xenopus* embryos. ß-Catenin (1.0 ng) or Wnt8 (50 pg) mRNA was injected into the ventral side of 4-cell stage embryos and total ß-catenin levels achieved at blastula stage were estimated by immunofluorescence on cryosections. A. Diagram of crossection of a blastula embryo indicating the areas used to compare ß-catenin staining. B, C. Ventral-animal and dorsal regions of uninjected embryos. Arrows: nuclear ß-catenin. Arrowheads: plasma membranes. D. Ventral region from Wnt8-injected embryo. Note the increased nuclear signal. E. Ventral region from ß-catenin-injected embryo. Note the very strong signal throughout the cells. F. Same field recorded with a 5 times shorter exposure time. G. Comparison of dorsalizing activity of Wnt and ß-catenin in early Xenopus embryos. The degree of dorsalization obtained was scored at tailbud stage. The phenotypes were classified in five categories of increasing dorsalization: normal, partial duplicated axis, complete duplicated axis, complete duplicated axis with shorten axis indicating partial global dorsalization and completely dorsalized, i.e. global dorsalization with reduced or no axis and radial head structures. p value according to χ2 test.

nuclear accumulation of ß-catenin strongest in the dorsal side, but also spread throughout the prospective mesoderm, while the signal remains lower in the ectoderm (Schohl and Fagotto, 2002; Schohl and Fagotto, 2003). With 50 pg Wnt8 mRNA, which is in excess of the amount required to induce complete dorsalization, ß-catenin nuclear levels were found to be only slightly higher than levels induced by the endogenous pathway (Fig. 4). However, the levels of exogenous ß-catenin corresponding to induction of a secondary axis were well beyond physiological levels, both in the cytoplasm and in the nucleus. These observations indicate that exogenous ß-catenin is less effective at activating the pathway than endogenous ß-catenin regulated by Wnt signals, consistent with the hypothesis that Wnt-induced ß-catenin is qualitatively different.

Quantitative differences in dephospho-ß-catenin plasma membrane labeling in Wnt responding tissues *in vivo*

Our data in the isogenic Kep1 and Kp6 cell lines demonstrate that dephospho-ß-catenin is recruited to the plasma membrane in response to Wnt stimulation in an E-cadherin independent fashion. Such an unbiased analysis would not be feasible in other *in vitro* model systems such as the commonly used colon cancer cell lines, where the Wnt pathway is constitutively active and E-cadherin expression varies even amongst subclones of low-expressing cell lines such as LS174T (unpublished data). We find that in our model system the increase in dephospho-ß-catenin is subtle and not detectable *in situ* in an E-cadherin +/+ background. However, based on earlier data in the *Drosophila* system from the Wieschaus lab (see below) we optimized our staining protocol for the detection of dephospho-ß-catenin in other systems as well. As a first approach we double-stained *Xenopus* embryo sections for total and dephospho-ß-catenin (Fig. 5). We detected a clear signal for dephospho-ß-catenin at the plasma membrane of mesodermal cells, but less in ectodermal cells (Fig 5B). Wnt over-expression led to membrane recruitment of dephospho-ß-catenin in ectodermal cells (Fig 5A) and increased membrane staining of total ß-catenin. Despite the fact that this model system lacks the advantage of an E-cadherin negative background, the observations in a physiological setting of a quantitative difference in (dephospho-)ß-catenin accumulation at the plasma membrane in Wnt responding versus Wnt non-responding cells are in agreement with the observations in our initial model system not suffering from this drawback. In order to unam-

4
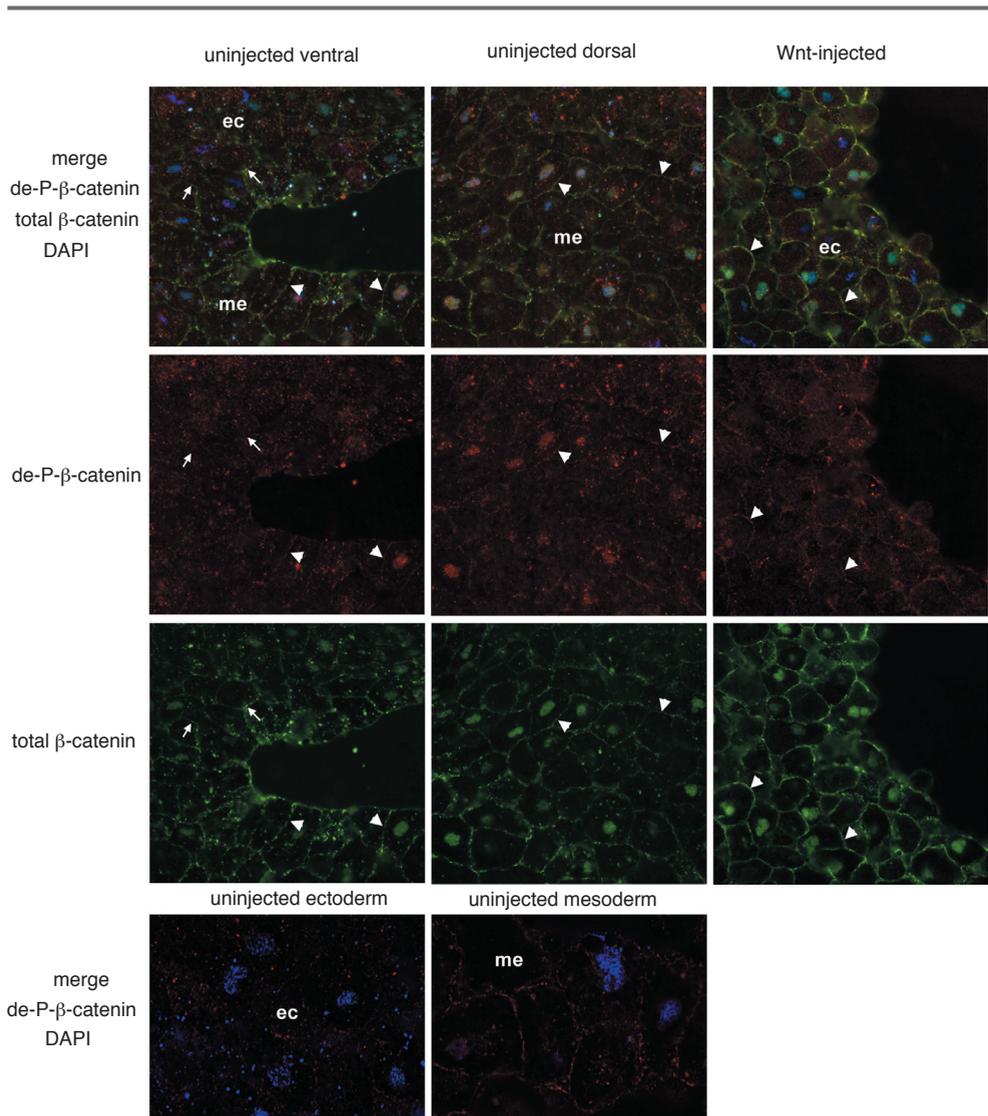
Figure 5. Membrane localization of dephospho-ß-catenin in the early *Xenopus* embryo. Cryosections of stage 9 embryos were stained for dephospho-ß-catenin (ABC) and total ß–catenin (H102) and nuclei were counterstained with DAPI. A. Selected fields of the ventral presumptive ectoderm and mesoderm (uninjected ventral), dorsal mesoderm (uninjected dorsal), and ventral ectoderm of an embryo injected with 50 pg Wnt8 mRNA (Wnt-injected). In uninjected embryos, ABC stains the outlines of mesodermal cells (me) (arrowheads) but not ectodermal cells (ec) (arrows). Membrane ABC is detected in ectodermal cells of Wnt-injected embryos (arrowheads). Small bright cytoplasmic spots seen all three color channels correspond to autofluorescent pigment granules. B. Higher magnification view of ABC staining of ectodermal (ec) and mesodermal (me) cells of uninjected cells. These two images were obtained by collection of z-stacks followed by 2D-nearest neighbors diconvolution and merge of 10 images from each stack.

biguously assign translocation of Wnt-induced dephospho-ß-catenin as E-cadherin-independent however, an E-cadherin negative background is required. We point out that the results on dephospho-ß-catenin plasma membrane accumulation in response to Wnt stimulation in the *Xenopus* model system parallel earlier data obtained in *Drosophila* where Wg signaling similarly
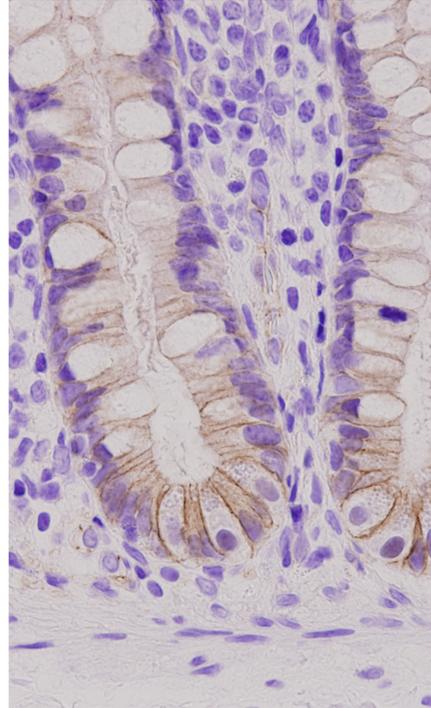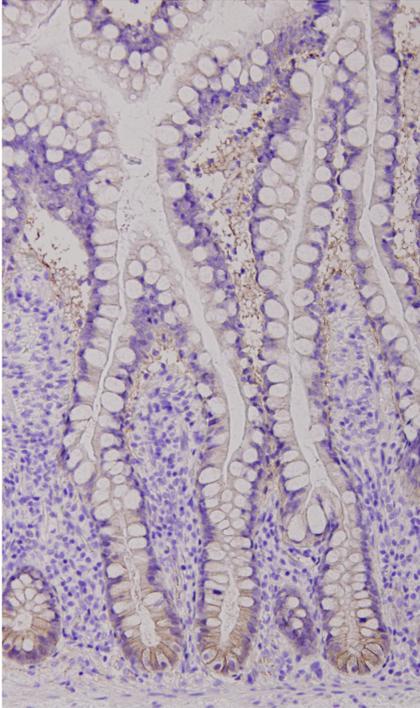
Figure 6. Dephospho-ß-catenin is enriched on the plasma membrane in human intestinal crypts. A. Low-power photomicrograph of a normal human small intestinal crypt-villus axis. Dephospho-ß-catenin is enriched on the crypt epithelial plasma membrane when compared to the plasma membrane labeling on differentiated villus cells. B. High-power photomicrograph of crypt compartment shown in A. Crypt epithelial cells including the presumptive intestinal epithelial stem cells or crypt base columnar (CBC) cells (Barker et al., 2007) show robust plasma membrane labelling.

4

increases plasma membrane levels of Armadillo (the fly ß-catenin homologue) in Wg-responding stripe regions, in addition to elevating cytosolic ,levels of the protein (Peifer et al., 1994b). This suggests that an increase in Armadillo at the plasma membrane is important for endogenous Wg signaling in the fruit fly as well.

We also tested Wnt-induced dephospho-ß-catenin plasma membrane enrichment in a second *in vivo* model of Wnt signaling. The intestinal epithelium of the human small intestine is organized into flask-shaped invaginations called crypts and finger-like projections termed villi. Wnt signaling has been shown to be essential for maintaining stem cell turn-over in the intestinal crypt (Korinek et al., 1998). We stained normal human small intestinal epithelium for dephospho-ß-catenin and found that similar to the situation in *Xenopus*, dephospho-ß-catenin is enriched at the plasma membrane of Wnt-responsive crypt epithelial cells when compared to differentiated cells on the villus epithelium (Fig. 6, Chapter 3,

Fig 3A and B).

We emphasize that it remains to be tested whether in these two *in vivo* examples of Wnt signaling, the plasma membrane localization of (dephospho-)β-catenin, which coincides with regions of known Wnt activity, represents the E-cadherin-independent signaling competent form, as this form could still potentially be masked.

Discussion

The currently prevailing model of Wnt signal transduction specifies that upon receipt of a Wnt ligand at the membrane-associated receptor complex, ß-catenin proteolysis is prevented and the protein accumulates in the cytosol. It has remained unclear how cytosolic destruction complexes sense ligand engagement at the plasma membrane. Recent studies have shown that Wnt treatment induces the formation of LRP6 co-receptor aggregates at the plasma membrane

(Bilic et al., 2007). These receptor aggregates in turn promote the recruitment of canonical Wnt pathway components including dishevelled, Axin and GSK3ß (Bilic et al., 2007; Schwarz-Romond et al., 2007). These observations parallel earlier data obtained in the *Drosophila* system where similarly recruitment of pathway components to the plasma membrane has been recorded upon activation of the pathway (Cliffe et al., 2003). How the inhibition of ß-catenin proteolysis ties up with the formation of these LRP6 signalosomes and whether ß-catenin itself may translocate to the plasma membrane along with its canonical destruction complex members is unknown. Here we show using an *in vitro* model system, that endogenous dephosphorylated ß-catenin indeed appears on the plasma membrane upon Wnt3A treatment. This translocation occurs independent of E-cadherin and dephosphorylated ß-catenin co-localizes at the plasma membrane with phospho-LRP6, Axin and APC. Together, our results suggests that Wnt signal transduction may be regulated at multiple levels other than, or in addition to, the inhibition of breakdown and that routing of *de novo* synthesized ß-catenin through the Wnt receptor complex is required for optimal transcriptional activity of the protein. This step in the processing of signaling-competent ß-catenin may have remained difficult to detect so far due to plasma membrane masking by the junctional pool of ß-catenin. We note that the punctate plasma membrane labeling observed in our model system bears a striking resemblance to the plasma membrane labeling described in the former studies (Bilic et al., 2007; Schwarz-Romond et al., 2007). In contrast to what has been described in these studies however, our plasma membrane enrichment appeared to occur at a later time-point. With regards this temporal difference, we stress that in contrast to these studies using overexpression assays to achieve stoichiometric amounts of destruction complex members, we have focused on the endogenous fraction of Wnt-responsive dephosphorylated ß-catenin only which, as we show, is relatively minor.

We propose that under normal physiological conditions, ß-catenin is activated at the plasma membrane upon Wnt stimulation, generating a signaling competent form. In line with this, Gottardi and Gumbiner have shown that Wnt stimulation generates a monomeric form of ß-catenin that selectively binds TCF and not E-cadherin (Gottardi and Gumbiner, 2004). Therefore, the activation step may constitute this transition. Plasma membrane activation is not absolutely required for signal transduction, as increasing ß-catenin to supraphysiological levels by interfering with its degradation will lead to transactivation as well. It will be important to test this hypothesis by studying the routing of Wnt-induced ß-catenin at endogenous levels.

Previous work in *X. laevis* has generated evidence for the notion that ß-catenin stability alone may not explain Wnt signaling outcome (Guger and Gumbiner, 2000; Nelson and Gumbiner, 1999). Later studies from the Wieschaus lab in the fly embryo using hypomorphic Armadillo alleles show that modulation of Wg signaling can occur in the presence of uniformly high levels of Armadillo (Tolwinski et al., 2003; Tolwinski and Wieschaus, 2001; Tolwinski and Wieschaus, 2004). Moreover, studies in cultured mammalian cell lines show that receptor-mediated signal transduction events such as Wnt stimulation or secreted Frizzled related protein (sFRP) inhibition can impinge on Wnt signaling output even in the presence of downstream mutations preventing ß-catenin breakdown (He et al., 2005; Suzuki et al., 2004). We are currently in the process of studying potential post-translational modifications on ß-catenin employing the E-cadherin -/- Kep1 cell line.

A model of ß-catenin activation at the receptor complex would allow ß-catenin output to be regulated on a direct stoichiometic 'per molecule' basis, in theory allowing one Wnt molecule to liberate a predetermined quanta of signaling-competent ß-catenin molecules. If correct, this regulation would be considerably more efficient than the currently proposed models in which Wnt signaling input is titrated against the activity of cytoplasmic degradation complexes to regulate gene expression in the nucleus. Regulation at multiple levels is similarly observed in the Hedgehog signal transduction pathway where stabilization of the transcriptional co-activator does not suffice for full activation (Methot and Basler, 1999). It is currently not known what mediates this activation step in Hedgehog signal transduction at the plasma membrane (Hooper and Scott, 2005). Regulation at multiple levels beyond the mere inhibition of proteolysis would allow the Wnt pathway to join other developmental pathways such as the Hedgehog and Notch signaling pathways, where the transcriptional co-activator is licensed for signaling at the plasma membrane.

Acknowledgements

Materials and Methods

Data analysis
Statistical analysis was done using the R software package (R Development Core Team, 2005).

Cell culture, transfection and reporter assays
SK-BR-3, Kep1 (E-cadherin-/-, p53 -/-), Kp6 (E-cadherin +/+, p53 -/-), SW480, LS174T, Colo320, HCT15, Colo205 and SW48 were cultured in DMEM supplemented with 10% fetal calf serum and penicillin/streptomycin (Gibco-BRL) and were transfected using Fugene-6 (Roche) as instructed by the supplier. 1×10^5 cells were transfected with 300 ng TOP/FOP-TK-luc, 1.5 ng pRL-CMV, 325 ng ΔNLRP6, 50 or 100 ng ß-Catenin, 10 ng Wnt1 and 50 ng H2B-mRFP. Luciferase reporter activity was measured 24 hours after transfection in SK-BR-3. 24 hours after transfection with Top/Fop-TK-luc, Kep1 cells were stimulated with Wnt3A for 7 hours, after which luciferase activity was measured using the Dual-Luciferase Reporter Assay System (Promega).

APC antibodies
Domains of mouse APC, termed APC-A (amino acids 788-1038), APC-B (amino acids 2170-2394), and APC-C (amino acids 2644-2845), were fused to GST and purified in bacteria. Rabbit polyclonal antisera were prepared as described (Hoogenraad et al., 2000). Rat monoclonal antibodies against APC were generated by Absea (China) using the same GST fusion proteins. Hybridomas were first tested for specific recognition of the respective GST fusion proteins. Positive clones (51 hybridomas for APC-A, 44 hybridomas for APC-B, and 58 hybridomas for APC-C) were subsequently tested on Western blot for recognition of eCFP-tagged APC domains and by immunofluorescence for detection of endogenous APC. We screened 9 rabbit polyclonals against the A, B and C domains, but none of the rabbit polyclonal antibodies were monospecific (data not shown). We subsequently screened 51 antibody-producing rat hybridomas for APC-A (amino acids 788-1038), 44 hybridomas for APC-B (amino acids 2170-2394) and 58 hybridomas for APC-C (amino acids 2644-2845). Two rat monoclonal antibodies (13F7, APC-A-derived, and 3E7, APC-B-derived) detected both overexpressed, eCFP-tagged APC (Supplementary Figure S2 C), as well as endogenous APC on Western blots (Supplementary Figure S2 D). These antibodies also recognized GFP-tagged full length APC in transfected COS-1 cells (data not shown) and endogenous APC in different cell lines (Figure S2 D and data not shown). As 3E7 recognized clusters of full length APC in MDCK cells, and not in SW480 cells that contain truncated APC (Supplementary Figure S2 E, F), we conclude that 3E7 detects endogenous APC in immunofluorescence studies.

Other antibodies and reagents
Further antibodies used were against ß-Catenin (C19220) (Transduction Labs) and H-102 (Santa Cruz), active ß-Catenin (ABC 8E7), Actin (Ab-1, Oncogene), N-Axin (Fagotto), E-cadherin (C20820, Transduction Labs), pan-cadherin (C3678, Sigma), Tp1479 LRP6 (Niehrs), M2 mAb FLAG (Sigma). Purified recombinant Wnt3A was a kind gift from R. Nusse (Stanford, CA) or obtained from R&D Systems. 4',6-diamidino-2-phenylindole (DAPI) and Actinomycin D were obtained from Sigma.

Plasmids
Top/Fop-TK, pRL-CMV and pRK5SK-ß-catenin were described before (Hendriksen et al., 2005) and ΔN-LRP6 was a kind gift from H. Clevers (Hubrecht laboratory, Utrecht, The Netherlands).

Western blotting
Proteins were analyzed by SDS-polyacrylamide gel electrophoresis (25 μg per lane) and Western blotting using Immobilon-P transfer membrane (Millipore). Aspecific sites were blocked with 5% skim milk (Oxio, Hampshire, England) at room temperature for one hour. Note that detection of dephospho-ß-catenin with the αABC antibody was inhibited by certain brands/lots of skim milk. Primary antibodies were incubated in 1% skim milk for 2 hours at room temperature in the following dilutions: E-cadherin 1:1500; ß-Catenin mAb C19220 1:5000, ABC 1:500; Actin 1:5000; mFLAG M2 1:500. Blots were washed with phosphate buffered saline (PBS)/0.05% Tween 20. Enhanced chemiluminescence (Amersham) was used for detection of proteins.

Immunofluorescence and confocal microscopy
For immunofluorescence, cells were grown on glass coverslips coated with fibronectin (Sigma) and fixed in 3.7% formalin in PBS for 10 min and permeabilized for 5 min in 0.2% Triton/PBS. For antigen retrieval, cells were incubated in 10 mM citric acid buffer pH 6 at 95°C for 20 min and blocked in 5% BSA/PBS at room temperature

4

for 10 min. Primary antibodies were incubated for 2 hours in 1% purified BSA/PBS using the following dilutions; ABC 1:200; total ß-Catenin C19220 1:250; total ß-Catenin H102 1:65; N-Axin 1:50; N-APC 1:100; APC 3E7 1:100; p-LRP6 1:250; LRP6 1:300; pan-cadherin 1:5000. Cells were shortly washed in PBS and incubated in fluorescently conjugated secondary antibodies (Molecular Probes) and DAPI in 1% BSA/PBS for 30 min, washed shortly in PBS and mounted in Mowiol. Images were recorded using a Leica NT, SP2 or SP2 AOBS confocal microscope.

Embryo injections and immunofluorescence

4-cell stage embryos were injected in one ventral blastomere with 25 or 50 pg Wnt8 mRNA or 1000 pg myc-tagged ß-catenin mRNA as previously described (Fagotto et al., 1996). Stage 9 embryos were fixed in 3-4% paraformaldeyde and sections were prepared and stained as previously described (Schohl and Fagotto, 2002). Antibodies used were total anti-ß-catenin H102 diluted 1:50, ABC 1:250, and secondary goat Alexa546/Alexa488 anti-rabbit/anti-mouse (Molecular Probes). Images were recorded with a Leica microscope using a narrow Cy3 filter and a 20x oil immersion objective.

Immunohistochemistry

Sections (4 µm) were deparaffinized and antigen retrieval was carried out by 10 min of boiling in 10 mM Tris/1 mM EDTA (pH 9). Subsequently slides were immersed in 0.3% hydrogen peroxide in methanol for 30 min and nonspecific binding was blocked with 5% normal goat serum for 1 hr at room temperature. The sections were incubated for 1 hr at room temperature in primary antibodies against total ß-Catenin (C19220 Transduction Labs) and active ß-Catenin (ABC 8E7). The Ultravision antipolyvalent HRP detection system (Lab Vision Corp., Fremont, CA, USA) was used to visualize antibody binding sites with 3,3'-diaminobenzidine as a chromogen. Sections were counterstained with hematoxylin.

References

Anderson, C. B., Neufeld, K. L. and White, R. L. (2002). Subcellular distribution of Wnt pathway proteins in normal and neoplastic colon. Proc Natl Acad Sci U S A 99, 8683-8.

Barker, N., van Es, J. H., Kuipers, J., Kujala, P., van den Born, M., Cozijnsen, M., Haegebarth, A., Korving, J., Begthel, H., Peters, P. J. et al. (2007). Identification of stem cells in small intestine and colon by marker gene Lgr5. Nature 449, 1003-7.

Bilic, J., Huang, Y. L., Davidson, G., Zimmermann, T., Cruciat, C. M., Bienz, M. and Niehrs, C. (2007). Wnt induces LRP6 signalosomes and promotes dishevelled-dependent LRP6 phosphorylation. Science 316, 1619-22.

Brocardo, M., Nathke, I. S. and Henderson, B. R. (2005). Redefining the subcellular location and transport of APC: new insights using a panel of antibodies. EMBO Rep 6, 184-90.

Cadigan, K. M. and Liu, Y. I. (2006). Wnt signaling: complexity at the surface. J Cell Sci 119, 395-402.

Cadigan, K. M. and Nusse, R. (1997). Wnt signaling: a common theme in animal development. Genes Dev 11, 3286-305.

Clevers, H. (2006). Wnt/beta-catenin signaling in development and disease. Cell 127, 469-80.

Cliffe, A., Hamada, F. and Bienz, M. (2003). A role of Dishevelled in relocating Axin to the plasma membrane during wingless signaling. Curr Biol 13, 960-6.

Davidson, G., Wu, W., Shen, J., Bilic, J., Fenger, U., Stannek, P., Glinka, A. and Niehrs, C. (2005). Casein kinase 1 gamma couples Wnt receptor activation to cytoplasmic signal transduction. Nature 438, 867-72.

Derksen, P. W., Liu, X., Saridin, F., van der Gulden, H., Zevenhoven, J., Evers, B., van Beijnum, J. R., Griffioen, A. W., Vink, J., Krimpenfort, P. et al. (2006). Somatic inactivation of E-cadherin and p53 in mice leads to metastatic lobular mammary carcinoma through induction of anoikis resistance and angiogenesis. Cancer Cell 10, 437-49.

Fagotto, F., Funayama, N., Gluck, U. and Gumbiner, B. M. (1996). Binding to cadherins antagonizes the signaling activity of beta-catenin during axis formation in Xenopus. J Cell Biol 132, 1105-14.

Gottardi, C. J. and Gumbiner, B. M. (2004). Distinct molecular forms of beta-catenin are targeted to adhesive or transcriptional complexes. J Cell Biol 167, 339-49.

Guger, K. A. and Gumbiner, B. M. (2000). A mode of regulation of beta-catenin signaling activity in Xenopus embryos independent of its levels. Dev Biol 223, 441-8.

He, B., Reguart, N., You, L., Mazieres, J., Xu, Z., Lee, A. Y., Mikami, I., McCormick, F. and Jablons, D. M. (2005). Blockade of Wnt-1 signaling induces apoptosis in human colorectal cancer cells containing downstream mutations. Oncogene 24, 3054-8.

Hoogenraad, C. C., Akhmanova, A., Grosveld, F., De Zeeuw, C. I. and Galjart, N. (2000). Functional analysis of CLIP-115 and its binding to microtubules. J Cell Sci 113 (Pt 12), 2285-97.

Hooper, J. E. and Scott, M. P. (2005). Communicating with Hedgehogs. Nat Rev Mol Cell Biol 6, 306-17.

Kobayashi, M., Honma, T., Matsuda, Y., Suzuki, Y., Narisa-

wa, R., Ajioka, Y. and Asakura, H. (2000). Nuclear translocation of beta-catenin in colorectal cancer. Br J Cancer 82, 1689-93.

Korinek, V., Barker, N., Moerer, P., van Donselaar, E., Huls, G., Peters, P. J. and Clevers, H. (1998). Depletion of epithelial stem-cell compartments in the small intestine of mice lacking Tcf-4. Nat Genet 19, 379-83.

Logan, C. Y. and Nusse, R. (2004). The Wnt signaling pathway in development and disease. Annu Rev Cell Dev Biol 20, 781-810.

McCrea, P. D., Turck, C. W. and Gumbiner, B. (1991). A homolog of the armadillo protein in Drosophila (plakoglobin) associated with E-cadherin. Science 254, 1359-61.

Methot, N. and Basler, K. (1999). Hedgehog controls limb development by regulating the activities of distinct transcriptional activator and repressor forms of Cubitus interruptus. Cell 96, 819-31.

Miyashiro, I., Senda, T., Matsumine, A., Baeg, G. H., Kuroda, T., Shimano, T., Miura, S., Noda, T., Kobayashi, S., Monden, M. et al. (1995). Subcellular localization of the APC protein: immunoelectron microscopic study of the association of the APC protein with catenin. Oncogene 11, 89-96.

Nelson, R. W. and Gumbiner, B. M. (1999). A cell-free assay system for beta-catenin signaling that recapitulates direct inductive events in the early xenopus laevis embryo. J Cell Biol 147, 367-74.

Peifer, M., Pai, L. M. and Casey, M. (1994a). Phosphorylation of the Drosophila adherens junction protein Armadillo: roles for wingless signal and zeste-white 3 kinase. Dev Biol 166, 543-56.

Peifer, M., Sweeton, D., Casey, M. and Wieschaus, E. (1994b). wingless signal and Zeste-white 3 kinase trigger opposing changes in the intracellular distribution of Armadillo. Development 120, 369-80.

Schohl, A. and Fagotto, F. (2002). Beta-catenin, MAPK and Smad signaling during early Xenopus development. Development 129, 37-52.

Schohl, A. and Fagotto, F. (2003). A role for maternal beta-catenin in early mesoderm induction in Xenopus. Embo J 22, 3303-13.

Schwarz-Romond, T., Metcalfe, C. and Bienz, M. (2007). Dynamic recruitment of axin by Dishevelled protein assemblies. J Cell Sci 120, 2402-12.

Staal, F. J., Noort Mv, M., Strous, G. J. and Clevers, H. C. (2002). Wnt signals are transmitted through N-terminally dephosphorylated beta-catenin. EMBO Rep 3, 63-8.

Suzuki, H., Watkins, D. N., Jair, K. W., Schuebel, K. E., Markowitz, S. D., Chen, W. D., Pretlow, T. P., Yang, B., Akiyama, Y., Van Engeland, M. et al. (2004). Epigenetic inactivation of SFRP genes allows constitutive WNT signaling in colorectal cancer. Nat Genet 36, 417-22.

Tolwinski, N. S., Wehrli, M., Rives, A., Erdeniz, N., DiNardo, S. and Wieschaus, E. (2003). Wg/Wnt signal can be transmitted through arrow/LRP5,6 and Axin independently of

Zw3/Gsk3beta activity. Dev Cell 4, 407-18.

Tolwinski, N. S. and Wieschaus, E. (2001). Armadillo nuclear import is regulated by cytoplasmic anchor Axin and nuclear anchor dTCF/Pan. Development 128, 2107-17.

Tolwinski, N. S. and Wieschaus, E. (2004). A nuclear function for armadillo/beta-catenin. PLoS Biol 2, E95.

van de Wetering, M., Barker, N., Harkes, I. C., van der Heyden, M., Dijk, N. J., Hollestelle, A., Klijn, J. G., Clevers, H. and Schutte, M. (2001). Mutant E-cadherin breast cancer cells do not display constitutive Wnt signaling. Cancer Res 61, 278-84.

van Noort, M., Meeldijk, J., van der Zee, R., Destree, O. and Clevers, H. (2002). Wnt signaling controls the phosphorylation status of beta-catenin. J Biol Chem 277, 17901-5.

van Noort, M., Weerkamp, F., Clevers, H. C. and Staal, F. J. (2007). Wnt signaling and phosphorylation status of beta-catenin: importance of the correct antibody tools. Blood 110, 2778-9.

Willert, J., Epping, M., Pollack, J. R., Brown, P. O. and Nusse, R. (2002). A transcriptional response to Wnt protein in human embryonic carcinoma cells. BMC Dev Biol 2, 8.

Zeng, X., Tamai, K., Doble, B., Li, S., Huang, H., Habas, R., Okamura, H., Woodgett, J. and He, X. (2005). A dual-kinase mechanism for Wnt co-receptor phosphorylation and activation. Nature 438, 873-7.

4
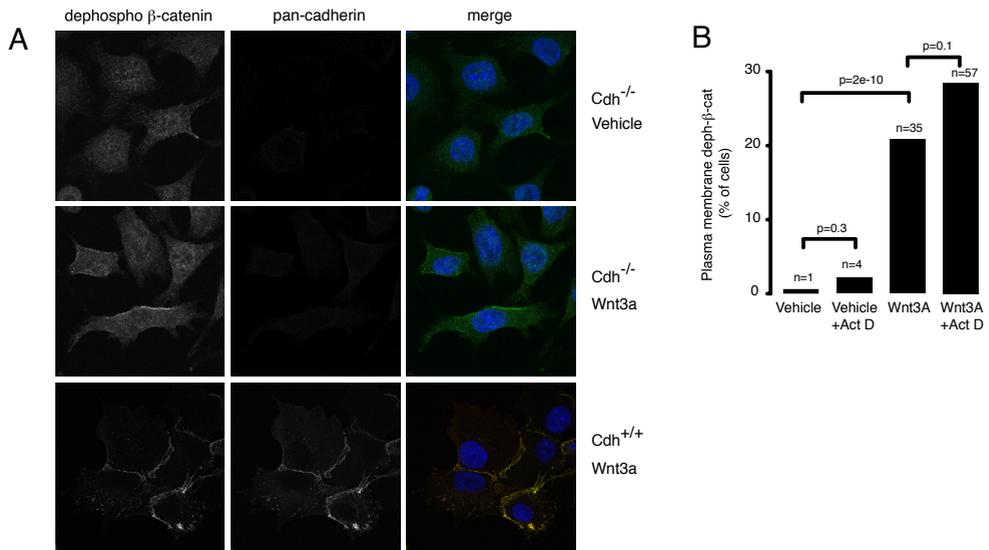
Figure S1 A. Membrane localization of dephospho-ß-catenin does not coincide with membrane localization of cadherins. Cells were stimulated as in A and stained for dephospho-ß-catenin and cadherins using a pan-cadherin antiserum. As a reference, E-cad +/+ cells are used. B. Plasma membrane recruitment of dephospho-ß-catenin is independent of ongoing transcription. E-cadherin -/- cells were analyzed as in A in the presence or absence of the transcription inhibitor Actinomycin D at 4 µg/ml. No significant difference in plasma membrane localization of dephospho-ß-catenin was observed. P values according to Fisher's exact tests.

Figure S2 Generation of anti-APC antisera. A. Domain structure of APC. Coiled coil and basic regions are shown as dark grey boxes at the N- and C-terminal ends of APC, respectively. Armadillo repeats (light blue), and ß-catenin (yellow and green) and axin (red) binding regions are also depicted. The domains (amino acids indicated) used to make GST fusion proteins are shown above the sequence. B - D. Western blot analysis. In (B) a blot is shown of overexpressed eCFP, and eCFP-tagged APC-A, -B, and -C in COS-1 cells. Proteins were detected with anti-GFP antibodies. In (C) a blot is shown of eCFP-APC-A (left panel) or eCFP-APC-B (right panel), overexpressed in COS-1 cells, and detected with 5 rat monoclonals against APC-A or with 5 monoclonals against APC-B. Note that only some antibodies recognize the eCFP-tagged proteins. Strips incubated with 13F7 and 3E7 are indicated. In (D) blots are shown with indicated cell lysates. Of the 4 cell lines used only HCT116 expresses full length APC (indicated as wt). The amino acids at which APC is truncated in the other cell lines are indicated. Note that 3E7 only recognizes full length APC (and degradation products), while 13F7 recognizes both full length and truncated forms of APC (E, F) on immunofluorescence. In (E) SW480 and MDCK cells were fixed and stained with the indicated antibodies (IN: polyclonal rabbit antibody donated by Inke Nathke). APC is found clustered in peripheral domains (indicated by arows). Note that 3E7 fails to stain such clusters in SW480 cells. In (F) a double labelling of 3E7 with anti-tubulin antibodies was performed. APC is concentrated at the ends of a subset of microtubules (arrows). The staining patterns obtained with 3E7 and 13F7 are comparable to that obtained with the IN antibody and resemble published patterns.

A

788-1038   2170-2394   2644-2845
    A   B   C

mAPC

B

eGFP-APC-A
eGFP-APC-B
eGFP-APC-C
eGFP
w

C

13F7   3E7

GFP-APC-A   GFP-APC-B

D

kDa   M   SW480 (1338)   CaCo2 (1367)   DLD-1 (1416)   HCT116 (wt)   SW480 (1338)   CaCo2 (1367)   DLD-1 (1416)   HCT116 (wt)

250 →

200 →

13F7   3E7

E

SW480   MDCK

13F7   IN

3E7   3E7

F

MDCK

3E7

merge

tubulin

4

87